Biomedicine & Pharmacotherapy 92 (2017) 69–77

Available online at
ScienceDirect
www.sciencedirect.com

Elsevier Masson France
EM|consulte
www.em-consulte.com/en

Original article

Anti-inflammatory and antioxidant effect of cerium dioxide nanoparticles immobilized on the surface of silica nanoparticles in rat experimental pneumonia

Z. Serebrovska[a,*], R.J. Swanson[b], V. Portnichenko[a], A. Shysh[a], S. Pavlovich[a], L. Tumanovska[a], A. Dorovskych[c], V. Lysenko[d], V. Tertykh[e], Y. Bolbukh[e], V. Dosenko[a]

[a] Bogomoletz Institute of Physiology, National Academy of Sciences, 4 Bogomoletz St., Kyiv 01024, Ukraine
[b] Liberty University College of Osteopathic Medicine in Lynchburg, 306 Liberty View Lane, Lynchburg, VA24502, USA
[c] Integrative Medicine Clinic "SmartMed", 16 Luteranska St., Kyiv, 01024, Ukraine
[d] Lashkariov Institute of Semiconductor Physics, National Academy of Sciences, 41 Nauki Ave., 03028, Kyiv, Ukraine
[e] Chuiko Institute of Surface Chemistry, National Academy of Sciences, 17 Generala Naumova St., 03164, Kyiv, Ukraine

ARTICLE INFO

Article history:
Received 4 March 2017
Received in revised form 4 May 2017
Accepted 12 May 2017

Keywords:
Anti-inflammatory
Antioxidant
Cerium dioxide nanoparticles
Metabolism
Silica nanoparticles
TNF-α
Il-6
CINC-2
Oxygen consumption

ABSTRACT

A massage with the potent counter-inflammatory material, cerium dioxide nanoparticles, is promising and the antioxidant properties of CeO_2 are considered the main, if not the only, mechanism of this action. Nevertheless, the elimination of ceria nano-particles from the organism is very slow and there is a strong concern for toxic effect of ceria due to its accumulation. To overcome this problem, we engineered a combined material in which cerium nanoparticles were immobilized on the surface of silica nanoparticles (CeO_2 NP), which is shown to be easily removed from an organism and could be used as carriers for nano-ceria. In our study particle size was 220 ± 5 nm, Zeta-potential −4.5 mV (in water), surface charge density −17.22 μC/cm^2 (at pH 7).

Thirty-six male Wistar rats, 5 months old and 250–290 g were divided into four groups: 1) control; 2) CeO_2 NP treatment; 3) experimental pneumonia (i/p LPS injection, 1 mg/kg); and 4) experimental pneumonia treated with CeO_2 NP (4 times during the study in dosage of 0.6 mg/kg with an orogastric catheter). Gas exchange and pulmonary ventilation were measured four times: 0, 1, 3 and 24 h after LPS injection in both untreated and CeO_2 NP-treated animals. The mRNA of TNF-α, Il-6, and CxCL2 were determined by RT-PCR. ROS-generation in blood plasma and lung tissue homogenates were measured by means of lucigenin- and luminol-enhanced chemiluminescence.

Endotoxemia in the acute phase was associated with: (1) pathological changes in lung morphology; (2) increase of ROS generation; (3) enhanced expression of CxCL2; and (4) a gradual decrease of $V^{\bullet}O_2$ and $V^{\bullet}_E$. CeO2 NP treatment of intact animals did not make any changes in all studied parameters except for a significant augmentation of $V^{\bullet}O_2$ and $V^{\bullet}_E$. CeO_2 NP treatment of rats with pneumonia created positive changes in diminishing lung tissue injury, decreasing ROS generation in blood and lung tissue and decreasing pro-inflammatory cytokine expression (TNF-α, Il-6 and CxCL2). Oxygen consumption in this group was increased compared to the LPS pneumonia group.

In our study we have shown anti-inflammatory and antioxidant effects of CeO_2 NP. In addition, this paper is the first to report that CeO_2 NP stimulates oxygen consumption in both healthy rats, and rats with pneumonia. We propose the key in understanding the mechanisms behind the phenomena lies in the property of CeO_2 NP to scavenge ROS and the influence of this potent antioxidant on mitochondrial function. The study of biodistribution and elimination of CeO_2NP is the purpose of our ongoing study.

1. Introduction

Biological properties of cerium dioxide nanoparticles (CeO_2 NP) have recently gained attention in different fields of bio-medical research. Biological activity of CeO_2 NP depends on particle shape, size, lattice features, and technology of production [1–3].

* Corresponding author.
E-mail address: belyak-serebrovska@hotmail.com (Z. Serebrovska).

http://dx.doi.org/10.1016/j.biopha.2017.05.064
0753-3322/

Two trends can be traced in the total volume of publications dedicated to CeO_2 NP: (1) the toxicity of CeO_2, which is contained in the metabolic byproducts, and other contaminates that can accumulate in tissues, especially in the lungs and liver, causing damage [4–6]; and (2) the potential application of CeO_2 NP in agriculture and medicine. One possible application is anti-cancer treatment since data have shown CeO_2 NP to be toxic to cancer cells while displaying minimal toxicity to normal tissues [7–9]. Several *in vitro* studies support the cytoprotective efficacies of CeO_2 NP in cardiac cells [10], monocytes [11], and pancreatic cells [12].

Publications of potent counter-inflammatory action of CeO_2 NP are promising as shown *in vivo* in peritonitis [13,14], sepsis [15], age-related macular degeneration [16], light damaged retina [3], and others. Antioxidant properties of CeO_2 are indicated as the main, if not the only mechanism for this effect [17–19]. The antioxidant potential of CeO_2 NP is high and comparable to the powerful agent superoxide dismutase [20]. As a regular antioxidant, CeO_2 NP diminishes oxidative disruption of membranes and scavenging superoxide decreases attraction of macrophages and neutrophils in inflamed tissue [21].

Recently published data show that due to its antioxidant properties, CeO_2 NPs are able to provide restoration of cell energy supplies when there is an increase of an external reactive oxygen species (ROS) load [22]. Mitochondrial membrane potential loss, calcium flux, decrease of the NADH/NAD ratio and ATP concentration caused by H_2O_2 treatment of primary cortical cells were restored by introduction of CeO_2 NP [23]. We assume that CeO_2 NP can improve energy production also in other physiological and pathological conditions.

Potential clinical application of nano-ceria is promising, nevertheless, the elimination of ceria nano-particles from the organism is very slow [24] and there is a strong concern for toxic effect of ceria due to it accumulation [25]. Some authors consider the ability of CeO_2 to be accumulated in tissues as a promising property since once introduced, CeO_2 can remain in damaged cells for a long time, continuing its cytoprotective work [1]. Nevertheless, accumulation of CeO_2 in tissues in uncontrolled concentration is dangerous since higher doses of CeO_2 NP become toxic. To overcome this problem, we engineered a combined material in which cerium nanoparticles were immobilized on the surface of silica nanoparticles. Because of their low toxicity and easy elimination from organisms, silica nanoparticles are widely used as nano-carriers for toxic drugs [26,27]. Here we describe a pilot study of new engineered particles, namely CeO_2 NP immobilized on commercially available spherical-shaped silica dioxide nanoparticles. In this combination nano-silica were used as potential safe CeO_2 nano-carrier.

We have made a model of lipopolysaccharides (LPS)-induced pulmonary inflammation in rats to study the effects of CeO_2 NP treatment evaluating lung morphology, ROS –production, expression of pro-inflammatory cytokines (tumor necrosis factor-α (TNF-α), interleykin-6 (IL6), chemokine (C-X-C motif) ligand 2(CxCL2)), oxygen uptake and other characteristics of lung ventilation.

2. Methods

The study protocol was approved by the Animal Care Ethics Committee of Bogomoletz Institute of Physiology, Kyiv, Ukraine. Male Wistar rats were maintainedin a 12 h light:dark cycle, with a temperature of 22 ± 3 °C. Food and water were available *ad libitum*.

2.1. Experimental pneumonia

We have chosen pneumonia induced by LPS specific to the cell membrane of *E. coli* as the model for our study. The presence of these structures in the tissues is recognized by the immune system as bacterial invasion which initiates an inflammation cascade. In our experiment LPS was administered *via* intraperitoneal (i.p.) injection. Pneumonia formed in this way is accompanied by sepsis [28–32].

Rats were injected i.p. with 1 mg/kg of LPS (*Escherichia coli* 055: B5; Sigma, St. Louis, MO, USA) dissolved in physiological saline, to induce endotoxaemia and lung inflammation.Controls were injected with sterile saline alone.

2.2. Study design

Thirty-six Wistar, 5 month old male rats, weighing 250–290 g were divided into four groups of 9 rats each: (1) control, (2) CeO_2 NP treatment, (3) experimental pneumonia, (4) experimental pneumonia treated with CeO_2 NP. Animals of all groups were sacrificed 24 h after pneumonia induction (LPS injection) and tissue samples were collected. The parameters of pulmonary ventilation and gas exchange were measured four times using a respiratory mask in conscious animals as follows: first before LPS injection (time zero), and then 1, 3 and 24 h after LPS injection. In control and healthy CeO_2 NP treated groups, pulmonary ventilation and gas exchange were both measured at these times with no additional treatment. 2,5% water solution of CeO_2 NP was administered 4 times during the study in dosage of 0.6 mg/kg with an orogastric catheter: first at time zero (for groups having pneumonia it was immediately prior to injection of LPS), and then at 1, 3 and 24 h after time zero.

2.3. Synthesis and characterization of particles

Synthesis of silica nanoparticles with immobilized cerium dioxide (CeO_2/SiO_2) was carried out as described in [33]. We used a deposition precipitation method *via* thermal treatment of deposited cerium hydroxide obtained by interaction of the dilute solutions of ammonium cerium (IV) nitrate $(NH_4)_2$ $Ce(NO_3)_6$ (Sigma-Aldrich) with ammonium hydroxide in the presence fumed silica nanoparticles (specific surface area of 300 m^2/g, Kalush Research Experimental Plant, Ukraine) all in solution. During thermal treatment at 623 K for 2 h, CeO_2 nanoparticles were formed and immobilized on a surface layer of highy-dispersed silica.The presence of CeO_2 nanoparticles was confirmed by X-ray

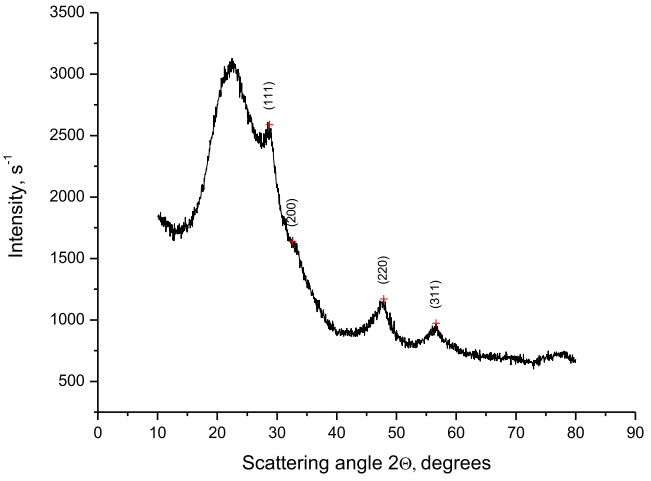

Fig. 1. X-ray diffraction pattern of cerium dioxide nanoparticles immobilized on silica particles. The XRD diffraction pattern indicated that the synthesized material contains particles of cerium dioxide (JCPDS card #34-0394). The crystallite's size was determined by the method for polycrystalline solids using the Scherrer equation. Per the data obtained, the average size of the nanoparticles of cerium dioxide deposited on the surface layer of our silica was 6–8 nm.

diffraction analysis (diffractometer DRON-4.7, Russia, CuK_α–irradiation) (Fig. 1).

Some surface characteristics (isoelectric point, surface charge density, Zeta potential) and average size of particles of the initial carrier (SiO_2) and particles with immobilized cerium dioxide (CeO_2/SiO_2) were estimated by a Zetasizer NanoZS^{TM}(Malvern Instruments, UK). These data are represented in Table 1. Surface charge densities of nanoparticles (σ) were measured in 0.01 M KCl solution at the dispersion concentration (*C*) of 3 mg/ml.

SiO_2 and CeO_2/SiO_2 particles sizes were estimated by a ZetasizerNanoZS^{TM}(Malvern Instruments, UK). Particles were dispersed in water (1 mg/ml) by ultrasound. Non-Invasive Back Scatter technology (NIBS) is incorporated to give the highest sensitivity simultaneously with the highest size and concentration range. Particles size was calculated as an average value from three scans which were performed without disturbing the initial water dispersion of the sample. The pH value was in the range of 5.2–6.0 (Fig. 2).

Significant increase in diameter of particles of CeO_2/SiO_2 samples presumably can occur due to essential changes of σ (Fig. 3) and Zeta-potential value (Table 1). Such characteristics can significantly reduce colloidal stability of water dispersions and thus the determined sizes correspond to conglomerates, not to single particles.

2.4. Histological analysis

All tissues were collected as 2–4 mm blocks, fixed in 10% neutral phosphate-buffered formalin for 24–48 h, dehydrated, cleared and embedded in paraffin. Four to five um sections were stained with hematoxylin and eosin (H&E) and evaluated with light microscopy (Scope: Nikon, Eclipse E-200, camera Nikon, ds-FI1) at 200, 400 and 1000x for morphological characteristics.

2.5. ROS generation

ROS generation in blood plasma and a lung tissue homogenate was measured by means of lucigenin- and luminol-enhanced chemiluminescence (CL). After decapitation, blood was gathered in a heparinized tube and immediately CL-assayed. Lung tissue homogenized on ice in a Potter-Elvehjem tissue grinder with 5 vol (w/v) of Hanks' balanced salt solution (100 mg/ml) without phenol red (HBSS). Samples for CL measurement contained the following ingredients in a total volume of 1 mL: 0.9 mL whole blood or lung tissue homogenate; 0.1 mL of 50 mM lucigenin or 0.1 mL of 20 mM luminol as the final concentration. After 3–5 min of spontaneous chemiluminescence, 0.1 mL of HBSS with 0.1 μg of opsonized zymosan (30 min incubation with rat serum at 37 °C) was added to enhance chemiluminescence. CL was then monitored for 15 min (Luminometer EA-1, Ukraine) at 37 °C and continuous mixing. The sum of light signals at a sampling frequency of 0.25 Hz was calculated and expressed as relative light units.

2.6. RNA isolation, reverse transcription, and real-time polymerase-chain reaction

Total RNA was isolated from lungs using the Trizol RNA-prep kit (Isogen, RussianFederation) according to the manufacturer's protocol. RNA concentration was determined using a NanoDrop spectrophotometerND1000 (NanoDrop Technologies Inc, USA).

Reverse transcription was performed using a RevertAid^{TM}H Minus First Strand cDNA Synthesis Kit (Fermentas, Germany),

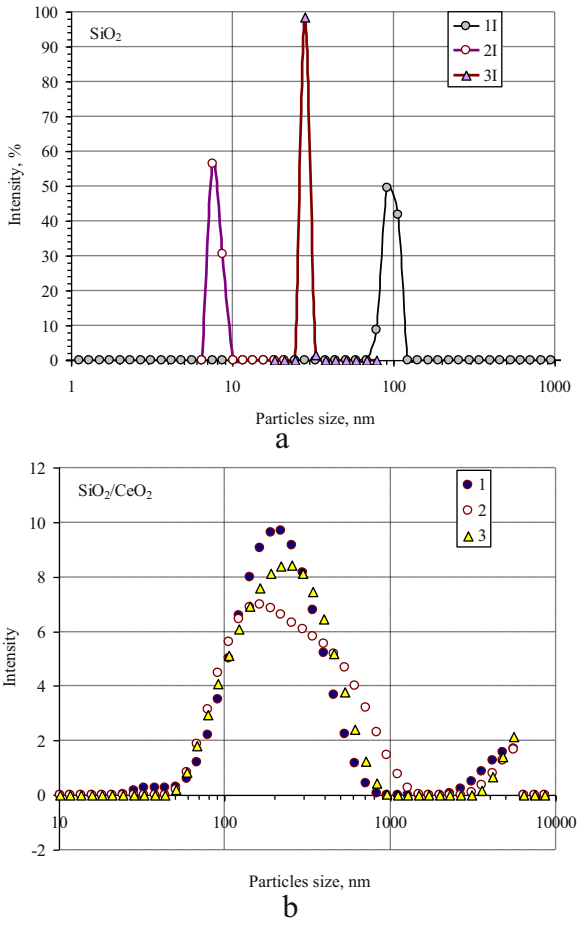

Fig. 2. Particles size distribution for SiO_2 (*a*) and CeO_2/SiO_2 (*b*) samples as a result of three successive measurements (curves 1I, 2I, 3I and 1, 2, 3, respectively) carried out for 10 min.

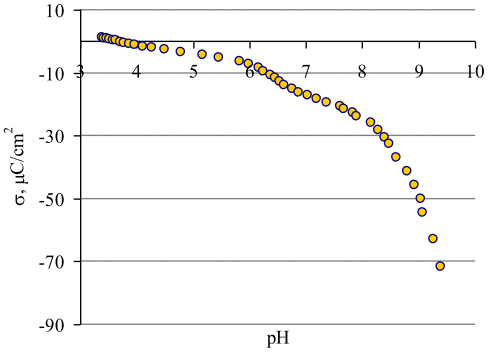

Fig. 3. Surface charge density of CeO_2/SiO_2particles at different pHvalues.

Table 1
Surface characteristics of particles of the initial carrier (SiO_2) and particles with immobilized cerium dioxide (CeO_2/SiO_2).

Sample	*C*, mg/ml	IEP, pH	Surfacecharge density μC/cm^2 (at pH 7)	Zeta-potential, mV (in water)	Particles size, nm (average)
SiO_2	3	2.40	−0,02	−7.6	56 ± 2
CeO_2/SiO_2	3	3.68	−17.22	−4.5	220 ± 5

using 1.2–1.5 μL of total RNA and random hexamerprimer. Received single-stranded DNA was used for real-time polymerase chain reaction (PCR).

2.7. Real-time PCR for mRNA expression of genes TNFa, IL6, CxCL2

We performed amplification in 10 μL of SYBR Green PCR Master Mix (Thermoscientific, USA)containing 20 pM of each primer. For amplifications of TNF-α, IL-6, CxCL2(corresponding toMIP2-

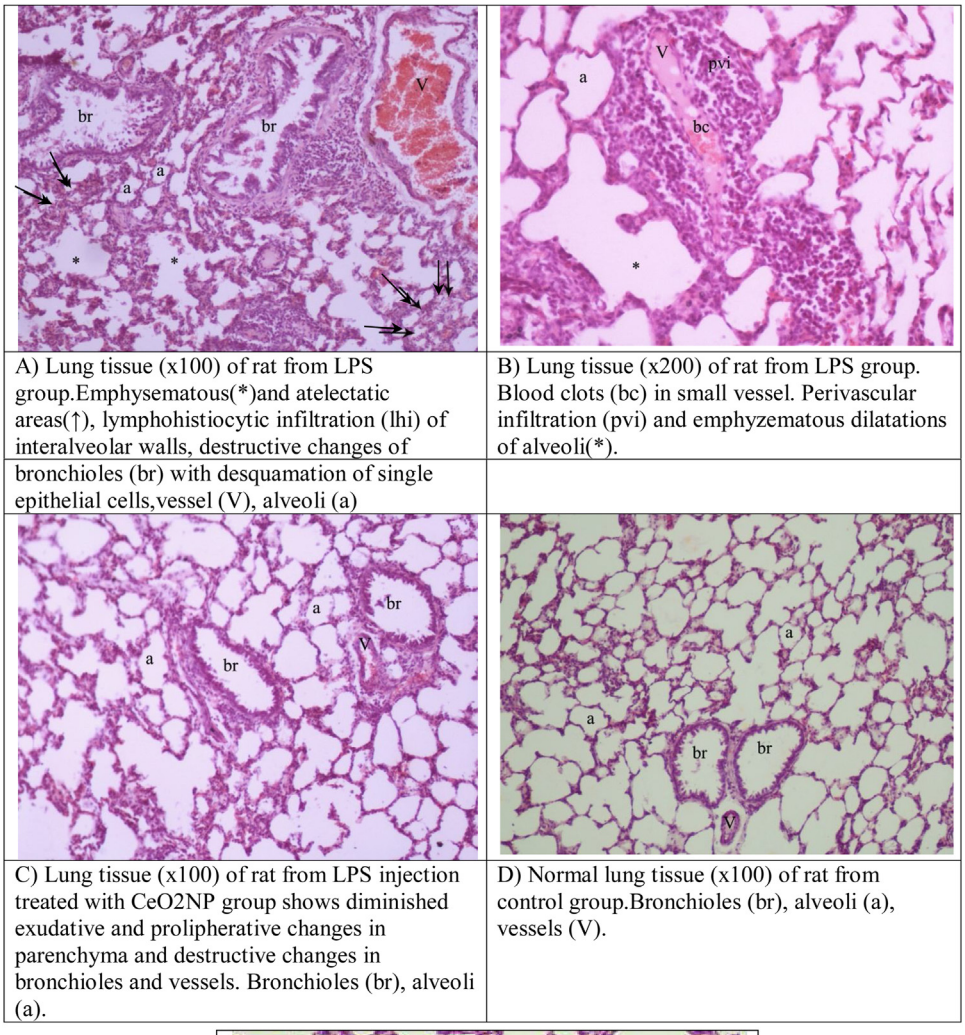

Fig. 4. Morphology of lung tissue of rats from different group.

alpha), and ACTB (corresponding to b-Actin, housekeeping gene) gene fragments, we used the following primers:

TNF-α Up: 5′-CCTCAGCCTCTTCTCATTCCT-3′
TNF-α Dw: 5′-GGGAACTTCTCCTCCTTGTTG-3′
IL6 Up: 5′-CAAGAGACTTCCAGCCAGTTG-3′
IL6 Dw: 5′-TGGGTGGTATCCTCTGTGAAG-3′
CxCL2 Up: 5′-AGGCTAACTGACCTGGAAAGG-3′
CxCL2 Dw: 5′-ATCAGGTACGATCCAGGCTTC-3′
ACTB Up: 50-TCATCACTATCGGCAATGAGC-30
ACTB Dw: 50-GGCCAGGATAGAGCCACCA-30

Sample volume was brought to 20 μL with deionized water. Amplification was performed on a 7500 Fast Real-Time PCR System ("Thermoscientific", USA). The amplification program consisted ofinitial AmpliTaq Gold_ DNA polymerase activation step at 95 °C for 10 min over the following 50 cycles: denaturation (95 °C for 15 s), annealing, and elongation (56 °C for 60 s). For control of specificity, we performed dissociation stage—sequential increase of temperature from 56 to 99 °C with registration of the drop in the double-stranded DNA-SYBR Green complexes fluorescence strength. We performed calculations using the 7500 Fast System SDS software provided. The cycle threshold is defined as the number of cycles required for the fluorescence signal to exceed the detection threshold. We calculated the expression of the target gene relative to the housekeeping gene as the difference between the threshold values of the two genes.

2.8. Respiration

The arrangement for measuring ventilatory and gas exchange parameters in rats included a one-way valved mask, a pneumotachograph for small laboratory animals with a pressure sensor, MPX5050, and a mass spectrometer type MH6202, Ukraine [34]. Signals from the pressure sensor and the mass spectrometer were processed by an analog-digital converter delivered to a computer and analyzed on the custom-written software. As was previously shown [34], the inertia of the mass spectrometer sensor does not affect measurement accuracy under respiratory rate lower than 150 breaths per min. Special calibration curves were used when the respiratory rate reached higher values.

We measured respiratory frequency (Freq), tidal volume (V_T) and calculated minute ventilation ($V^{\bullet}_E$). On the bases of expired O_2 and CO_2 curves we calculated rate of oxygen uptake per minute ($V^{\bullet}O_2$).

These data were expressed in mL/min/kg of body weight to BTPS (body temperature and pressure, saturated system) for respiratory volume and to STPD (standard temperature and pressure, dry system) for $V^{\bullet}O_2$. To exclude circadian metabolism oscillation influences on our results all measured parameters were compared with respective results from intact animals. Data are represented as % in comparison with control group.

3. Results and discussion

3.1. Morphological study

The introduction of CeO_2 NP to intact animals caused minor changes in lung tissue (Fig. 4E).

LPS injection alone led to primary injuries in lung tissue: (1) formation of emphysematous and atelectatic fragments; (2) pneumocytic dystrophy and loss; (3) bronchial epithelium desquamation; (4) vessel dilation; (5) damage of vessel walls; (6) perivascular edema; and (7) thrombosis. Thus, we conclude that intraperitoneal LPS injection (1 mg/kg) causes pulmonary inflammation in experimental rats (Fig. 4A and B).

Micrographs from the LPS-injected animals treated with CeO_2 NP showed fewer pneumocytes, bronchioles and vessel damages (Fig. 4C). These results support a reduced severity in the inflammatory process.

3.2. ROS generation

ROS generation in whole blood of rats from the CeO_2 NP group did not differ from the control (Fig. 5). LPS injection caused dramatic increase of ROS production in blood (by 554% compared to control), while in the LPS + CeO_2 NP group ROS was significantly lower (by 67% compared to the LPS group). Luminol-enhanced chemiluminescence reflects the total pool of ROS (O_2^-, $^{\bullet}OH$, H_2O_2 and other peroxides) generation, thus, CeO_2 NP treatment powerfully diminished oxidative stress induced by LPS. Interacting with macrophages, LPS initiates a positive feedback loop, involving cytokine expression, neutrophil and macrophage attraction, NAD (P)-H oxidase activation and ROS production. CeO_2 NP treatment limits one or more links in this process.

ROS production in lung tissue was similar to whole blood values. CeO2 NP treatment itself made some enhancement of ROS production, but these changes were statistically insignificant (Fig. 6). LPS injections caused enhancement of ROS production and the addition of CeO2 NP treatment of rats with pneumonia produced a statistically significant ($p < 0.05$) decrease of ROS.

LPS injections caused enhancement of ROS production and the addition of CeO_2 NP treatment of rats with pneumonia produced a significant ($p < 0.05$) decrease of ROS. In lung tissue homogenate, we measured lucigenin-enhanced chemiluminescence, which primarily reflects O_2^-, a major ROS product of mitochondria and activated neutrophils. LPS induces O_2^- production in lung tissue and CeO_2 NP treatment inhibits this process.

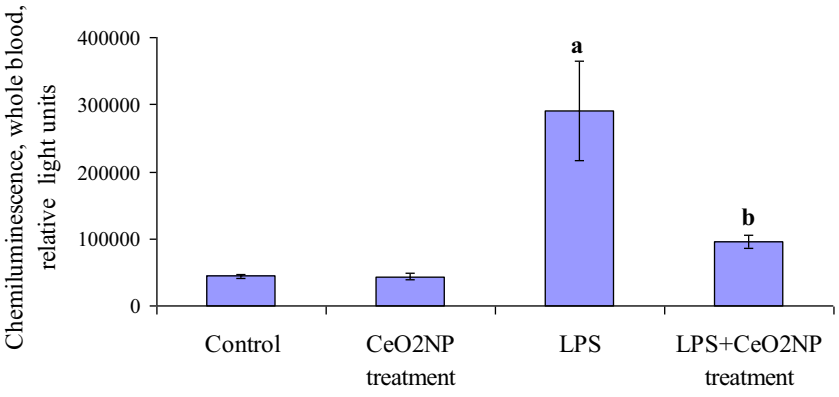

Fig. 5. Chemiluminescence of whole blood. *Values are means ± SE*, [a] $p < 0.05$ compared to control, [b] $p < 0.05$ compared to LPS group.

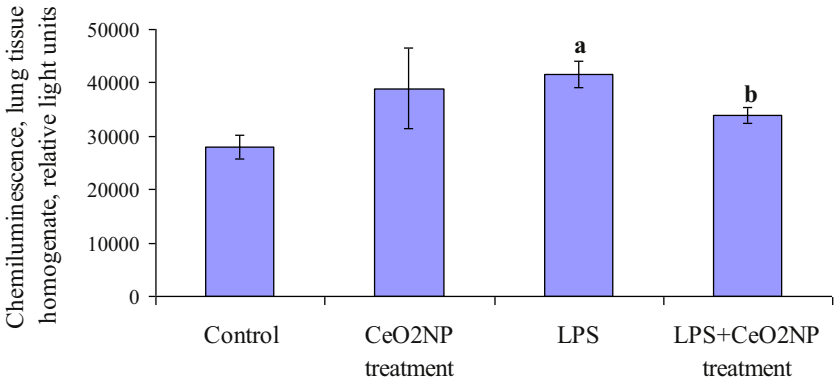

Fig. 6. Chemiluminescence of lung tissue homogenate. *Values are means ± SE*, [a] $p < 0.05$ compared to control, [b] $p < 0.05$ compared to LPS group.

3.3. Cytokine expression

We did not observe any differences of TNF-α, Il-6 and CxCL2 expression in the CeO_2 NP group in comparison with the control. LPS injection caused enhanced expression of CxCL2 (by 68%) while TNF-α and Il-6 remained unchanged. In the LPS + CeO_2 NP group, a significant decrease of TNF-α, Il-6 and CxCL2 expression was observed. The level of expression of all three cytokines was lower than the control but not statistically significant (Figs. 7–9).

3.4. Respiration

Treatment of intact rats with CeO_2 NP (CeO_2 NP group) caused an increase of $V^{\bullet}O_2$ at the 2nd and 3rd measurement. Values returned to baseline in the 4th measurement. Development of pneumonia in the LPS group caused gradual decrease of oxygen consumption with minimum values in the 4th measurement, 24 h after LPS injection (Fig. 10). In the LPS + CeO_2 NP group the $V^{\bullet}O_2$ did not differ from the control group in the 2nd measurement but then significantly increased in the 3rd measurement, returning to control levels in the 4th measurement. The superposition of two potent factors: pneumonia and CeO_2 NP treatment can be observed in this group. Nevertheless, CeO_2 NP treatment almost eliminated the effect of the LPS injection.

Changes in lung ventilation were similar to those in oxygen consumption. In the LPS group V_T was reduced in all measurements with minimal values obtained in the final measurement. In the CeO_2 NP group V_T increases with the most pronounced effect in the 2rd measurement (Fig. 11).

Changes in $V^{\bullet}_E$ were largely due to tidal volume changes. In the LPS + CeO_2 NP group, $V^{\bullet}_E$ in the 2nd and 3rd measurements with a decrease to baseline values in the 4th measurement (Fig. 12).

We can conclude that CeO_2NP increases oxygen consumption and lung ventilation in healthy rats and in animals with LPS pneumonia.

We noted a decrease of VO_2, V_T and $V^{\bullet}_E$ in the 4th measurement in the CeO_2 NP treated groups. The data patterns in the present study are a consequence of measuring the ventilatory and gas exchange parameters before the CeO_2NP introduction, 1 and 3 h after CeO_2 NP introduction and 21 h after the last introduction of CeO_2NP. The decreased metabolism in the 4th measurement in the CeO_2NP and LPS + CeO_2 NP groups would thus be due to the decrease in CeO_2NP concentration as a result of normal metabolic clearance from the animal's body. These results conform with the desirable properties for investigating nano particles: we combined cerium dioxide with silica to promote particle elimination and prevent accumulation in the organism. The pharmacodynamics of CeO_2NP s is the focus of our ongoing research. We have changed the experimental design, excluding the possibility of a habituation effect by introducing the experimental substance prior to all measurements.

Morphological analysis confirmed the development of pneumonia in rats after LPS injection. Observed pulmonary injury was associated with significant increase of ROS generation in blood and lung tissue and enhanced expression of the pro-inflammatory cytokine CxCl2. The development of pneumonia was also accompanied by a gradual decrease in oxygen consumption and lung ventilation, which is possibly related to lung function lesion, as well as to the inhibition of metabolism due to intoxication [35].

CeO_2NP treatment of intact animals has not created any changes in the lung morphology, in ROS generation or in cytokine expression. However, oxygen consumption and pulmonary ventilation were significantly increased: oxygen consumption was augmented by 70% an hour after the CeO_2NP introduction. More

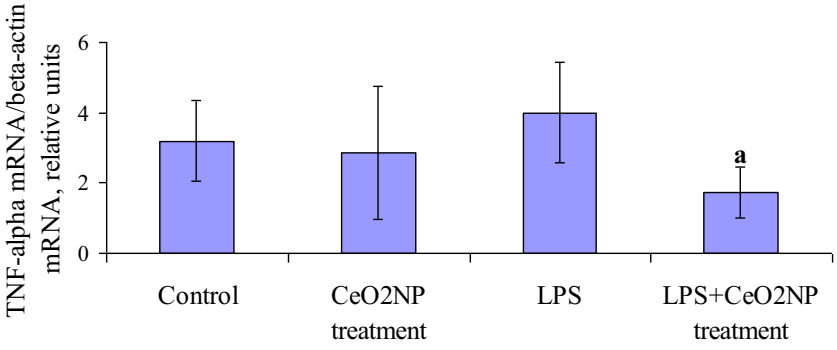

Fig. 7. Expression of TNF-alpha. *Values are means ± SE*, [a] $p = 0.05$ compared to LPS.

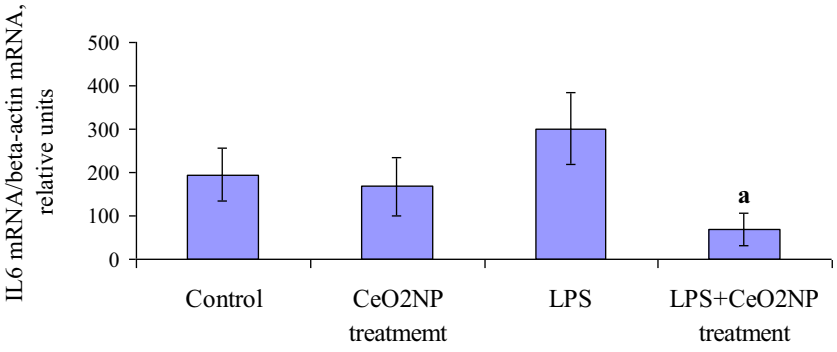

Fig. 8. Expression of IL-6. *Values are means* ± *SE*, $^{a}p < 0.05$ compared to LPS.

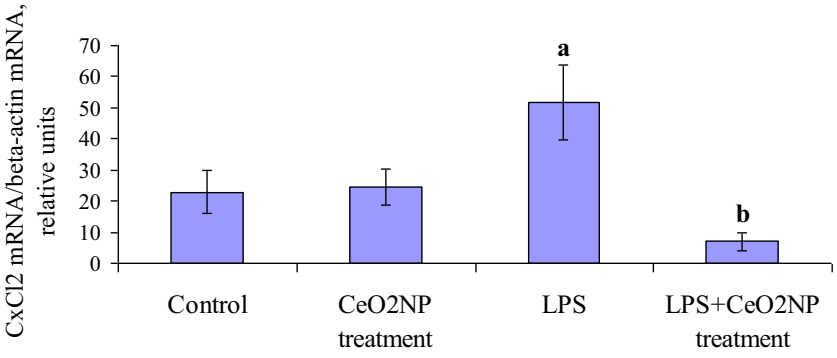

Fig. 9. Expression of CxCl2. *Values are means* ± *SE*, $^{a}p < 0.05$ compared to control, $^{b}p = 0.001$ compared to LPS group.

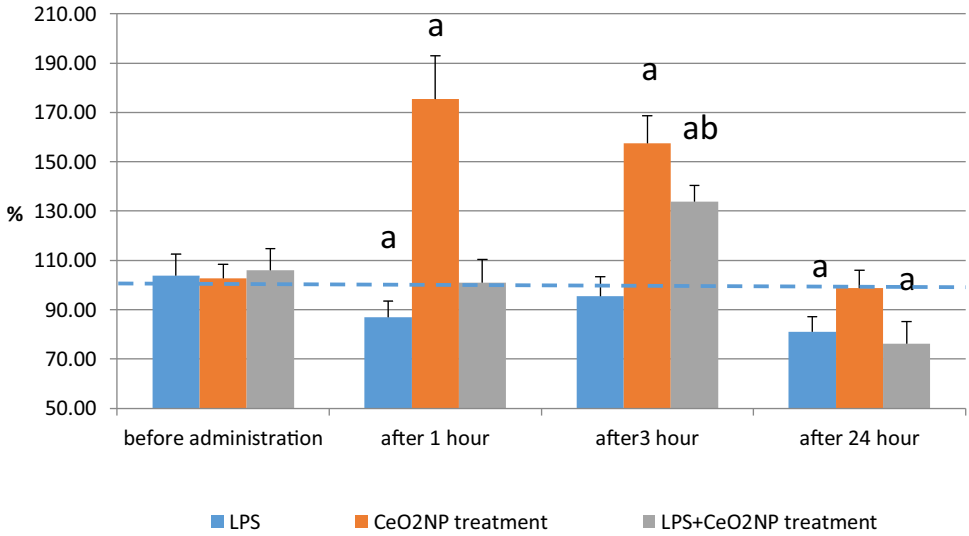

Fig. 10. Dynamic of $V^{\bullet}O_2$ in different groups. Data are represented as % in comparison with control group, indicated by dashed line. *Values are means* ± *SE*, $^{a}p < 0.05$ compared to control, $^{b}p < 0.05$ compared to LPS group.

intensive pulmonary ventilation would be expected to satisfy the enhanced demand of gas exchange.

CeO_2NP treatment of rats with pneumonia created positive changes: diminished lung tissue injury, decreased ROS generation in blood and lung tissue and pro-inflammatory cytokine expression of TNF-α, Il-6 andCINC-2. Oxygen consumption in this group was increased compared to LPS group: it did not differ from the control group in the 2nd measurement and was significantly higher, than in LPS group in the 3rd measurement. We assume a superimposition of the metabolic effect of CeO_2NP with depressed oxygen consumption due to acute pneumonia. Thus, CeO_2NP treatment partially eliminated the effect of the LPS injection.

Our data suggest that the counter-inflammatory effect of CeO_2NP is associated with antioxidant properties of this material. Prior research has shown a major regulatory role which ROS plays in the LPS inflammatory response. Introduction of antioxidant N-acetylcysteine suppressedLPS-inducedexpression ofpro-inflammatory cytokines in gingivalfibroblasts [36].

Metabolic effects of CeO_2NP should be associated with the scavenging of ROS produced in mitochondria. As mentioned,

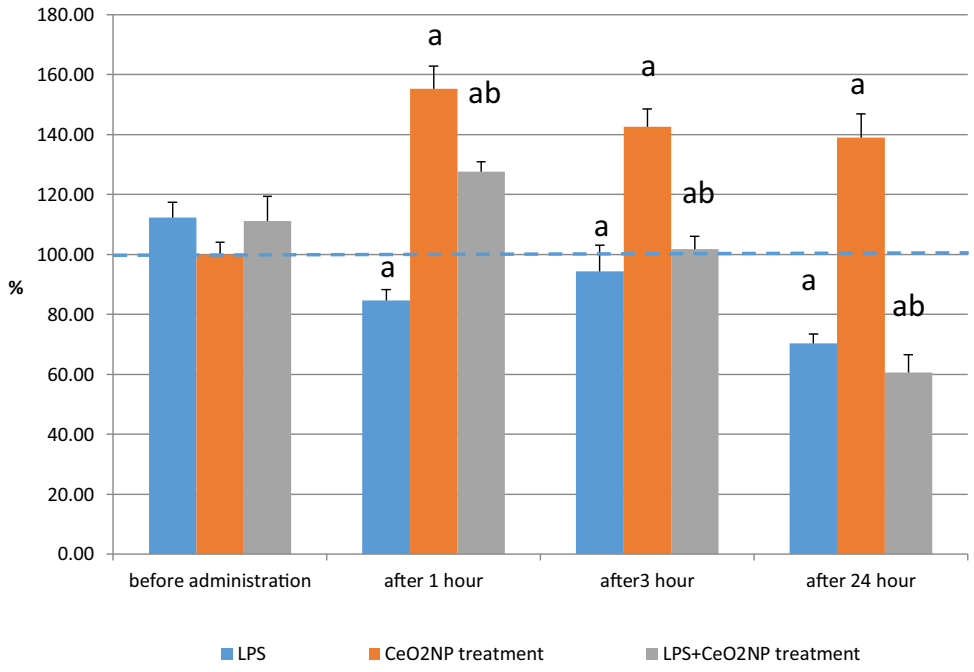

Fig. 11. Dynamic of V_T in different groups. Data are represented as % in comparison with control group, indicated by dashed line. *Values are means ± SE*, $^{a}p < 0.05$ compared to control, $^{b}p < 0.05$ compared to LPS group.

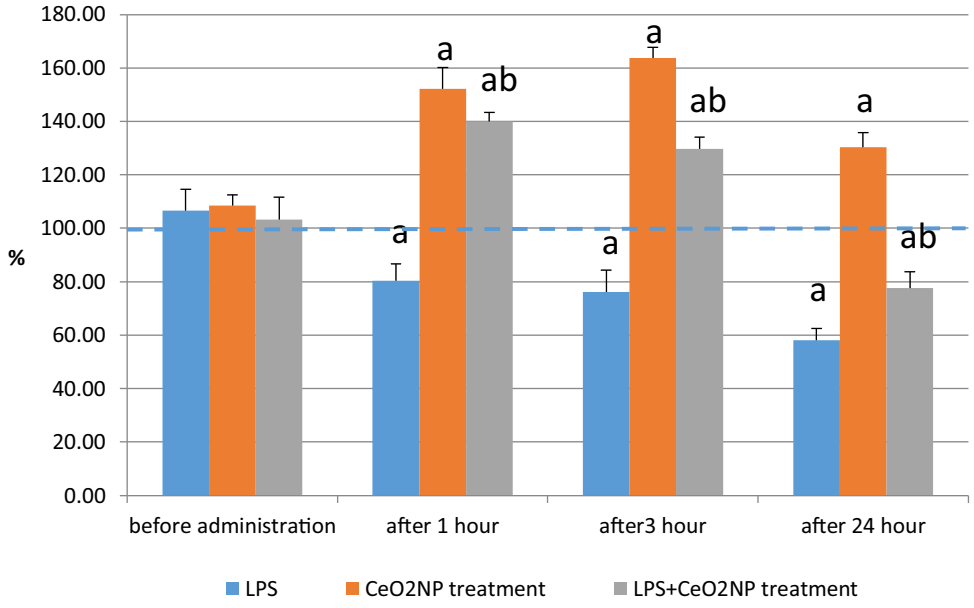

Fig. 12. Dynamic of $V^{\bullet}_E$ in different groups. Data are represented as % in comparison with control group, indicated by dashed line. *Values are means ± SE*, $^{a}p < 0.05$ compared to control, $^{b}p < 0.05$ compared to LPS group.

CeO_2NPs increases the mitochondrial membrane potential and ATP synthesis under the influence of ROS [23]. We assume that in our research, CeO_2NP affected the negative feedback mechanism in mitochondrial superoxide production.

Literature data suggest that after i/v introduction CeO_2 nano-particles accumulate mainly in liver and spleen, with less concentration in lung and kidneys [24]. The absorption of CeO_2 nanoparticles from gastro-intestinal tract is very low [37], that is why inhalation or i/v injections are used to obtain the effects of nano-ceria in organism. In our study we used silica nano-particles, which are shown to be well absorbed from intestine [38] as carrier for ceria. The biodistribution of silica nano-particles is similar to ceria [27], that is why we assume that our combined particles after absorption from gastrointestinal tract accumulate in different organs, including lungs, to make their biological effects.

Our study has shown that this new combined material produces effects which are similar to properties described for nano-ceria alone. The next step to possible clinical application of CeO_2NP is to prove, if this material conserves the qualities known for silica nano-particles and can be easily eliminated from an organism. The study of biodistribution and elimination of CeO_2NP is the purpose of our ongoing study.

We do not know yet the exact mechanism of obtained effects: presumably it can be the effect of ceria, whereas silica works exclusively as carrier, but we cannot exclude the possible effect of SiO2 itself, or in combination. Future investigations are needed to answer this question.

4. Conclusion

Our study has shown anti-inflammatory and antioxidant effect of CeO_2NP. In addition, we show that introduction of CeO_2NP stimulates oxygen consumption both in healthy rats, and in rats with pneumonia. We propose the key in understanding the mechanisms behind the phenomena lies in the property of CeO_2 NP to scavenge ROS and the influence of this potent antioxidant on mitochondrial function.

The study of biodistribution and elimination of CeO_2NP is the purpose of our ongoing study.

References

[1] N. Gravina, K. Maghni, M. Welman, L. Yahia, D.A. Mbeh, P.V. Messina, Protective role against hydrogen peroxide and fibroblast stimulation via Ce-doped TiO2 nanostructured materials, Biochim. Biophys. Acta 1860 (February (2)) (2016) 452–464.

[2] L. Fiorani, M. Passacantando, S. Santucci, S. Di Marco, S. Bisti, R. Maccarone, Cerium oxide nanoparticles reduce microglial activation and neurodegenerative events in light damaged retina, PLoS One 10 (October (10)) (2015) e0140387.

[3] J.M. Dowding, S. Das, A. Kumar, T. Dosani, R. McCormack, A. Gupta, T.X. Sayle, D. C. Sayle, L. von Kalm, S. Seal, W.T. Self, Cellular interaction and toxicity depend on physicochemical properties and surface modification of redox-active nanomaterials, ACS Nano 7 (June (6)) (2013) 4855–4868.

[4] Jane Ma, Robert R. Mercer, Mercer Barger, Diane Schwegler-Berry, Joel M. Cohen, Philip Demokritou, Vincent Castranova, Effects of amorphous silica coating on cerium oxide nanoparticles induced pulmonary responses, Toxicol. Appl. Pharmacol. 288 (Ocyober (1)) (2015) 63–73.

[5] K.M. Rice, S.K. Nalabotu, N.D. Manne, M.B. Kolli, G. Nandyala, R. Arvapalli, J.Y. Ma, E.R. Blough, Exposure to cerium oxide nanoparticles is associated with activation of mitogen-activated protein kinases signaling and apoptosis in rat lungs, J. Prev. Med. Public Health 48 (May (3)) (2015) 132–141.

[6] Lili Wang, Wenchao Ai, Yanwu Zhai, Haishan Li, Kebin Zhou, Huiming Chen, Effects of Nano-CeO_2 with different nanocrystal morphologies on cytotoxicity in HepG2Cells, Int. J. Environ. Res. Public Health 12 (September (9)) (2015) 10806–10819.

[7] Ying Gao, Kan Chen, Jin-lu Ma, Fei Gao, Cerium oxide nanoparticles in cancer, OncoTargets Ther. 7 (2014) 835–840.

[8] A. Asati, S. Santra, C. Kaittanis, J. Manuel Perez, Surface-charge-dependent cell localization and cytotoxicity of cerium oxide nanoparticles, ACS Nano 4 (September (9)) (2010) 5321–5331.

[9] M. Pešić, A. Podolski-Renić, S. Stojković, B. Matović, D. Zmejkoski, V. Kojić, G. Bogdanović, A. Pavićević, M. Mojović, A. Savić, I. Milenković, A. Kalauzi, K. Radotić, Anti-cancer effects of cerium oxide nanoparticles and its intracellular redox activity, Chem. Biol. Interact. 232 (May) (2015) 85–93.

[10] Jianli Niu, Kangkai Wang, Pappachan E. Kolattukudy, Cerium oxide nanoparticles inhibits oxidative stress and nuclear factor-κB activation in H9c2 cardiomyocytes exposed to cigarette smoke extract, J. Pharmacol. Exp. Ther. 338 (July (1)) (2011) 53–61.

[11] Salik Hussain, Faris Al-Nsour, Annette B. Rice, Jamie Marshburn, Brenda Yingling, Zhaoxia Ji, Jeffrey I. Zink, Nigel J. Walker, Stavros Garantziotis, Cerium dioxide nanoparticles induce apoptosis and autophagy in human peripheral blood monocytes, ACS Nano 6 (7) (2012) 5820–5829.

[12] Melissa S. Wason, Jimmie Colon, Soumen Das, Sudipta Seal, James Turkson, Jihe Zhao, H. Cheryl, Baker sensitization of pancreatic cancer cells to radiation by cerium oxide nanoparticle-induced ROS production, Nanomedicine 9 (May (4)) (2013) 558–569.

[13] S. Asano, R. Arvapalli, N.D. Manne, M. Maheshwari, B. Ma, K.M. Rice, V. Selvaraj, E.R. Blough, Cerium oxide nanoparticle treatment ameliorates peritonitis-induced diaphragm dysfunction, Int. J. Nanomed. 10 (2015) 6215–6225.

[14] N.D. Manne, R. Arvapalli, N. Nepal, T. Shokuhfar, K.M. Rice, S. Asano, E.R. Blough, Cerium oxide nanoparticles attenuate acute kidney injury induced by intra-abdominal infection in Sprague-Dawley rats, J. Nanobiotechnol. 13 (2015) 75.

[15] V. Selvaraj, N.D. Manne, R. Arvapalli, K.M. Rice, G. Nandyala, E. Fankenhanel, E. R. Blough, Effect of cerium oxide nanoparticles on sepsis induced mortality and NF-κB signaling in cultured macrophages, Nanomedicine (Lond.) 10 (8) (2015) 1275–1288.

[16] S.V. Kyosseva, L. Chen, S. Seal, J.F. McGinnis, Nanoceria inhibit expression of genes associated with inflammation and angiogenesis in the retina of Vldlr null mice, Exp. Eye Res. 116 (November) (2013) 63–74.

[17] R.M. Hashem, L.A. Rashd, K.S. Hashem, H.M. Soliman, Cerium oxide nanoparticles alleviate oxidative stress and decreases Nrf-2/HO-1 in D-GALN/LPS induced hepatotoxicity, Biomed. Pharmacother. 73 (July) (2015) 80–86.

[18] L.L. Wong, Q.N. Pye, L. Chen, S. Seal, J.F. McGinnis, Defining the catalytic activity of nanoceria in the P23H-1 rat, a photoreceptor degeneration model, PLoS One 10 (March (3)) (2015) e0121977.

[19] V.C. Minarchick, P.A. Stapleton, E.M. Sabolsky, T.R. Nurkiewicz, Cerium dioxide nanoparticle exposure improves microvascular dysfunction and reduces oxidative stress in spontaneously hypertensive rats, Front. Physiol. 6 (2015) 339.

[20] Y. Li, P. Li, H. Yu, Y. Bian, Recent advances (2010–2015) in studies of cerium oxide nanoparticles' health effects, Environ. Toxicol. Pharmacol. 44 (June) (2016) 25–29.

[21] D. González-Flores, M. De Nicola, E. Bruni, F. Caputo, A.B. Rodríguez, J.A. Pariente, L. Ghibelli, Nanoceria protects from alterations in oxidative metabolism and calcium overloads induced by TNFα and cycloheximide in U937 cells: pharmacological potential of nanoparticles, Mol. Cell. Biochem. 397 (December (1–2)) (2014) 245–253.

[22] J. Niu, A. Azfer, L.M. Rogers, X. Wang, P.E. Kolattukudy, Cardioprotective effects of cerium oxide nanoparticles in a transgenic murine model of cardiomyopathy, Cardiovasc. Res. 73 (3) (2007) 549–559.

[23] A. Arya, N.K. Sethy, M. Das, S.K. Singh, A. Das, S.K. Ujjain, R.K. Sharma, M. Sharma, K. Bhargava, Cerium oxide nanoparticles prevent apoptosis in primary cortical culture by stabilizing mitochondrial membrane potential, Free Radic. Res. 48 (July (7)) (2014) 784–793.

[24] R.A. Yokel, T.C. Au, R. MacPhail, S.S. Hardas, D.A. Butterfield, R. Sultana, M. Goodman, M.T. Tseng, M. Dan, H. Haghnazar, J.M. Unrine, U.M. Graham, P. Wu, E.A. Grulke, Distribution, elimination, and biopersistence to 90 days of a systemically introduced 30 nm ceria-engineered nanomaterial in rats, Toxicol. Sci. 127 (May (1)) (2012) 256–268, doi:http://dx.doi.org/10.1093/toxsci/kfs067 Epub 2012 Feb 23.

[25] F.R. Cassee, E.C. van Balen, C. Singh, D. Green, H. Muijser, J. Weinstein, K. Dreher, Exposure, health and ecological effects review of engineered nanoscale cerium and cerium oxide associated with its use as a fuel additive, Crit. Rev. Toxicol. 41 (March (3)) (2011) 213–229.

[26] A. Baeza, M. Vallet-Regí, Smart mesoporous silica nanocarriers for antitumoral therapy, Curr. Top. Med. Chem. 15 (22) (2015) 2306–2315.

[27] Changhui Fu, Tianlong Liu, Linlin Li, Huiyu Liu, Dong Chen, Fangqiong Tang, The absorption, distribution, excretion and toxicity of mesoporous silica nanoparticles in mice following different exposure routes, Biomaterials 34 (March (10)) (2013) 2565–2575.

[28] J. Qu, J. Zhang, J. Pan, L. He, Z. Ou, X. Zhang, X. Chen, Endotoxin tlerance inhibits lipopolysaccharide-initiated acute pulmonary inflammation and lung injury in rats by the mechanism of nuclear factor-kappaB, Scand. J. Immunol. 58 (December (6)) (2003) 613–619.

[29] R.B. Brauer, C. Gegenfurtner, B. Neumann, M. Stadler, C.D. Heidecke, B. Holzmann, Endotoxin-induced lung inflammation is independent of the complement membrane attack complex, Infect. Immun. 68 (March (3)) (2000) 1626–1632.

[30] R. Demiralay, N. Gürsan, H. Erdem, Regulation of sepsis-induced apoptosis of pulmonary cells by posttreatment of erdosteine and N-aceylcysteine, Toxicology 228 (December (2–3)) (2006) 151–161.

[31] A.C. Elder, R. Gelein, M. Azadniv, M. Frampton, J. Finkelstein, G. Oberdörster, Systemic effects of inhaled ultrafine particles in two compromised, aged rat strains, Inhal. Toxicol. 16 (June (6–7)) (2004) 461–471.

[32] L.H. Lancaster, J.W. Christman, T.R. Blackwell, M.A. Koay, T.S. Blackwell, Suppression of lung inflammation in rats by prevention of NF-kappaB activation in the liver, Inflammation 25 (February (1)) (2001) 25–31.

[33] Benjaram M. Reddy, Pranjal Saikia, Pankaj Bharali, Lakshmi Katta, Gode Thrimurthulu, Highly dispersed ceria and ceria–zirconia nanocomposites over silica surface for catalytic applications, Catal. Today 141 (2009) 109–114.

[34] V.P. Pozharov, Automatic installation for measuring the volume-time parameters of external respiration and gas exchange in small laboratory animals, Fiziol Zh 4 (2017) 119–121.

[35] M.C. Exline, E.D. Crouser, Mitochondrial mechanisms of sepsis-induced organ failure, Front. Biosci. 13 (May) (2008) 5030–5041.

[36] D.Y. Kim, J.H. Jun, H.L. Lee, K.M. Woo, H.M. Ryoo, G.S. Kim, J.H. Baek, S.B. Han, N-acetylcysteine prevents LPS-induced pro-inflamatory cytokines and MMP2 production in gingival fibroblsts, Arch. Pharm. Res. 30 (October (10)) (2007) 1283–1292.

[37] N.V. Konduru, R.J. Jimenez, A. Swami, S. Friend, V. Castranova, P. Demokritou, J. D. Brain, R.M. Molina, Silica coating influences the corona and biokinetics of cerium oxide nanoparticles, Part. Fibre Toxicol. 12 (2015) 31.

[38] C.M. Lee, T.K. Lee, D.I. Kim, Y.R. Kim, M.K. Kim, H.J. Jeong, M.H. Sohn, S.T. Lim, Optical imaging of absorption and distribution of RITC-SiO2 nanoparticles after oral administration, Int. J. Nanomed. 9 (December (Suppl. 2)) (2014) 243–250.